Published online May 16, 2005

2792–2805 *Nucleic Acids Research, 2005, Vol. 33, No. 9*
doi:10.1093/nar/gki557

Localization of spermine binding sites in 23S rRNA by photoaffinity labeling: parsing the spermine contribution to ribosomal 50S subunit functions

Maria A. Xaplanteri, Alexandros D. Petropoulos, George P. Dinos and Dimitrios L. Kalpaxis*

Laboratory of Biochemistry, School of Medicine, University of Patras, GR-26500 Patras, Greece

Received February 7, 2005; Revised and Accepted April 19, 2005

ABSTRACT

Polyamine binding to 23S rRNA was investigated, using a photoaffinity labeling approach. This was based on the covalent binding of a photoreactive analog of spermine, N^1-azidobenzamidino (ABA)-spermine, to *Escherichia coli* ribosomes or naked 23S rRNA under mild irradiation conditions. The cross-linking sites of ABA-spermine in 23S rRNA were determined by RNase H digestion and primer-extension analysis. Domains I, II, IV and V in naked 23S rRNA were identified as discrete regions of preferred cross-linking. When 50S ribosomal subunits were targeted, the interaction of the photoprobe with the above 23S rRNA domains was elevated, except for helix H38 in domain II whose susceptibility to cross-linking was greatly reduced. In addition, cross-linking sites were identified in domains III and VI. Association of 30S with 50S subunits, poly(U), $tRNA^{Phe}$ and AcPhe-tRNA to form a post-translocation complex further altered the cross-linking, in particular to helices H11–H13, H21, H63, H80, H84, H90 and H97. Poly(U)-programmed 70S ribosomes, reconstituted from photolabeled 50S subunits and untreated 30S subunits, bound AcPhe-tRNA in a similar fashion to native ribosomes. However, they exhibited higher reactivity toward puromycin and enhanced tRNA-translocation efficiency. These results suggest an essential role for polyamines in the structural and functional integrity of the large ribosomal subunit.

INTRODUCTION

The bacterial ribosome, a large ribonucleoprotein particle, consists of two unequal subunits designated 30S and 50S. The 50S subunit comprises two RNA species, 23S and 5S rRNA, and 33 proteins (1–3). The 23S rRNA from *Escherichia coli* is composed of 2904 nt and is subdivided into six major structural domains. Peptide bond formation and peptide release are catalyzed by the large subunit of the ribosome, where the peptidyltransferase (PTase) center is located (2). In addition to this center, the large subunit includes a factor-binding center, which triggers the GTPase activities of the G-protein factors involved in protein synthesis and mediates the conformational changes they all promote (4). Both subunits are involved in translocation, in which the tRNAs and mRNA precisely move through the intersubunit cavity, one codon at a time.

50S subunits, largely depleted of proteins, still exhibit PTase activity, indicating that 23S rRNA plays a principal role in catalysis (5). Recent crystallographic analysis has demonstrated that the PTase center is bare of proteins (6). This implies that peptide-bond formation as well as peptide release is catalyzed by RNA. However, a contribution from some ribosomal proteins cannot be completely excluded (4,7). Furthermore, monovalent and divalent cations as well as polycations, such as polyamines, are essential for the ribosome structure integrity and hence, for optimal translation efficiency. Despite the fact that much has been learned about the role and location of metal ions in ribosomes (8–16), there is still relatively little information (17–22) concerning the contacts between polyamines and the large ribosomal subunit. In fact, polyamines, such as spermine and spermidine, are essential for correct tRNA positioning to ribosomes (23) and regulation of ribosomal active centers (24–26). Also, it has been indicated by immuno-electron microscopy that polyamines are predominantly located in both free and attached ribosomes of the rough endoplasmic reticulum in mammalian cells (27). We have previously demonstrated in a cell-free system derived from *E.coli* that spermine not only promotes the formation and stabilization of the initiator ribosomal complex at 6 mM Mg^{2+}, but also causes a concentration-dependent allosteric biphasic effect on PTase activity; at low concentrations (<100 μM) stimulates the PTase activity, whereas at higher

*To whom correspondence should be addressed. Tel: +30 2610 996124; Fax: +30 2610 997690; Email: dimkal@med.upatras.gr

concentrations (>200 μM) causes partial noncompetitive inhibition (28). Recently, we found that the inhibition effect is at least partially due to a perturbation by spermine of the functional conformation of the donor substrate (29). On the contrary, the stimulatory effect seems to be related with the binding of spermine to ribosomes. As the tertiary structure of ribosome depends strongly on electrostatic forces, polyamines may simply facilitate the conformational rearrangements that correctly position the catalytic elements of ribosome, or may donate additional catalytic groups in *trans*. Obviously, to unveil the molecular basis of polyamine effects on the structure and function of the 50S subunit, the localization of polyamine binding sites on ribosomal proteins and 23S rRNA is a prerequisite. The former issue has been already settled (17–20); however, the latter has not been completely elucidated to date.

Although early studies suggested that endogenous spermine does not exist in *E.coli*, small amounts of spermine could be detected in these cells by more sensitive methods (30). *E.coli* cells employ an uptake system, which transports both spermidine and spermine into the cells. Including exogenous spermine at 15 μM in a synthetic growth-medium leads to accumulation of spermine (~36 μM) into a polyamine-requiring mutant of *E.coli*, MA261, and to a recovery of cell growth by >60%, compared with that obtained by the addition of 300 μM putrescine or 80 μM spermidine (31). This and other studies support the notion that all of the cellular functions of polyamines can be fulfilled by spermine. Owing to its four positive charges, spermine is the most effective of the naturally occurring polyamines in stabilizing the RNA folding. Nevertheless, spermine, like the other polyamines, is a small and flexible molecule and exchanges rapidly in the time scale of analytical methods. For instance, spermine is squeezed out of nucleic acid crystals during their preparation. On the other hand, among all ribosomal crystal structures reported to date, only the structure of the 50S subunit from *Haloarcula marismortui* has been analyzed at high enough resolution to allow the identification of bound polyamines. These and other arguments can explain the difficulties to detect spermine complexed with ribosomes in the form of crystals and the fact that crystallographic studies have been limited so far to only tRNA complexes with spermine (26). Despite the fact that NMR or computational techniques have recently offered direct evidence of cation binding pockets in RNA molecules, their applications have been limited to the detection of metal ion binding sites (32,33).

In the present study, mapping of spermine binding sites in 23S rRNA is achieved by a photoaffinity labeling approach in combination with RNase H digestion and primer-extension analysis. The rationale is that photoprobe cross-linking acts as a barrier for reverse transcriptase. This technique bypasses all disadvantages of other cross-linking methods utilizing homobifunctional reagents (17–19), and has been successfully applied so far for mapping spermine binding sites in AcPhe-tRNA bound to the P-site of poly(U)-programmed 70S ribosomes (29), in ribosomal proteins (20), or in 16S rRNA from *E.coli* (34). The results of the present study represent the first unambiguous and complete mapping of spermine binding sites in 23S rRNA. Identification of these sites should deepen our understanding of polyamine effects on ribosomal structure and function.

MATERIALS AND METHODS

Reagents and materials

Spermine tetrahydrochloride, spermidine trihydrochloride, dimethyl sulfate (DMS), DMS stop solution, heterogeneous tRNA from *E.coli*, puromycin dihydrochloride and thiostrepton from *Streptomyces azureus* were from Sigma (St Louis, MO). L-[2, 3, 4, 5, 6 ^{3}H] Phenylalanine and [γ-^{32}P]ATP were purchased from Amersham Biosciences Inc. (Piscataway, NJ). RNase H was obtained from Promega (Madison, WI) and AMV reverse transcriptase from Roche Diagnostics (Mannheim, Germany). dNTPs and ddNTPs were from Boehringer (Mannheim, Germany). N^1-azidobenzamidino (ABA)-spermine was synthesized and purified according to Clark *et al*. (35). Elongation factor G (EFG) from *E.coli* was kindly provided by Prof. K. H. Nierhaus. Cellulose nitrate filters (type HA; 0.45 μM pore size) were purchased from Millipore Corporation (Bedford, MA).

Biochemical preparations

Salt-washed (0.5 M NH_4Cl) and polyamine-depleted 70S ribosomes, native 50S and 30S ribosomal subunits, and partially purified translation factors were prepared from *E.coli* B cells as reported previously (20). 23S rRNA, 5S rRNA and total proteins (TP50) were isolated from 50S ribosomal subunits as shown in the same study. Prior to their use, rRNA or ribosomal subunits were activated in buffer 50 mM HEPES-KOH, pH 7.2, 20 mM magnesium acetate and 100 mM NH_4Cl, by incubation for 20 min at 42°C. Samples were then cooled to 0°C and the Mg^{2+} concentration was normalized to 6 mM. Ac[^{3}H]Phe-tRNA was prepared from heterogeneous *E.coli* tRNA, as described elsewhere (28). It was charged to 77%, 100% being 28 pmol of [^{3}H]Phe per A_{260} U (Sigma). Post-translocation complex of poly(U)-programmed ribosomes, complex C, containing $tRNA^{Phe}$ at the E-site and AcPhe[^{3}H]-tRNA at the P-site was prepared according to Dinos *et al*. (36). Complex C prepared in the absence of translation factors and photolabeled at 300 μM of photoprobe (condition A), or in the presence of translation factors and photolabeled at 50 μM of photoprobe (condition B), was charged with AcPhe-tRNA to 94 and 82%, respectively. When required, 50S ribosomal subunits modified by ABA-spermine were incubated for 30 min at 37°C with two molar equivalents of native 30S subunits in buffer containing 50 mM HEPES-KOH, pH 7.2, 15 mM magnesium acetate, 100 mM NH_4Cl and 6 mM 2-mercaptoethanol. Samples were cooled to 0°C, normalized at Mg^{2+} concentration equal to 6 mM and then used for complex C formation. Total reconstitution of 50S ribosomal subunits from TP50, 23S and 5S rRNA was achieved by a two-step incubation procedure (37).

Photoaffinity labeling and mapping of ABA-spermine cross-linking sites in 23S rRNA

Naked 23S rRNA, 50S ribosomal subunits or complex C were photolabeled with ABA-spermine and separated from excess photoprobe, as shown previously (34). The sites in 23S rRNA to which ABA-spermine was cross-linked were determined by a combination of two approaches; RNase H cleavage and primer-extension analysis. Namely, 23S rRNA covalently complexed with ABA-[^{14}C]spermine was digested with

RNase H in the presence of selected pairs of 11 deoxynucleotides complementary to sequences located at positions 200 nt apart in the primary structure of 23S rRNA. Thus, cleavage of 23S rRNA at sites that bracketed cross-links released a fragment which was tagged by covalently attached ABA-[^{14}C]spermine and, therefore, could be readily detected by electrophoretic and auto-radiographic analysis (34). Precise identification of the cross-linking sites was achieved by primer-extension analysis according to Stern *et al*. (38), making use of the fact that reverse transcriptase pauses or stops one position before a modified nucleoside by ABA-spermine. The stops of reverse transcriptase reaction were visualized on a gel autoradiogram. Only bands reproduced at least three times were taken into account. Controls with unmodified 23S rRNA or samples photolabeled in the simultaneous presence of a 250-fold excess of natural polyamines were run in parallel. Naked 23S rRNA, 50S ribosomal subunits or complex C, untreated or photolabeled, were modified with DMS as described previously (34).

Binding of Ac[^{3}H]Phe-tRNA to the ribosomal P- and A-sites

Binding was performed by incubating Ac[^{3}H]Phe-tRNA with poly(U)-programmed 70S ribosomes pre-filled (A-site binding) or not pre-filled (total binding) in their P-site by tRNA^{Phe} (34). The value of bound Ac[^{3}H]Phe-tRNA was measured by nitrocellulose filtration. The P-site bound Ac[^{3}H]Phe-tRNA was estimated from the total binding by titration with puromycin (2 mM, 2 min at 25°C).

Peptide bond formation assay

The PTase activity of complex C, untreated or photolabeled by ABA-spermine, was titrated by the puromycin reaction. The reaction was carried out at 25°C in buffer A (100 mM Tris–HCl, pH 7.2, 6 mM magnesium acetate, 100 mM NH_4Cl and 6 mM 2-mercaptoethanol) containing puromycin in excess (34). When required, 50 μM spermine was also included in the reaction mixture. The product, Ac[^{3}H]Phe-puromycin, was extracted in ethyl acetate and its radioactivity was measured in a liquid scintillation spectrometer. The product was expressed as the percentage (x) of complex C radioactivity added in the reaction mixture. The values of x, appropriately corrected (22), were fitted into Equation 1

$$\ln \frac{100}{100 - x} = k_{obs} \cdot t. \quad \mathbf{1}$$

The pseudo-first-order rate constant, k_{obs}, is related to the puromycin concentration, [S], by the relationship

$$k_{obs} = k_3[S]/(K_s + [S]), \quad \mathbf{2}$$

where k_3 represents the catalytic rate constant of PTase, and K_s the dissociation constant of the intermediate Michaelis–Menten complex between puromycin and complex C. The values of k_3 and K_s were estimated by non-linear regression fitting of k_{obs} and [S] values to Equation 2 (Microcal Origin, version: 5.00, provided by Microcal Software, Inc.).

Translocation assays

Pre-translocation ribosomal complex, containing tRNA^{Phe} at the P-site and Ac[^{3}H]Phe-tRNA at the A-site, was prepared according to Dinos *et al*. (36). Aliquots of the above complex were mixed with buffer A containing 0.015 μM EFG and 0.12 mM GTP. When desired, 50 μM spermine was also included in buffer A. The mixtures were incubated at 25°C for the indicated time intervals. Translocation was monitored by reaction with puromycin at 2 mM for 3 min (over 8 half-lives) at 25°C. The puromycin solution also contained thiostrepton at a final concentration of 5 μM (added from 5 mg/ml stock solution in dimethyl sulfoxide) to ensure that no translocation takes place during the puromycin reaction. Spontaneous translocation was measured in the absence of EFG. For EFG-dependent experiments, increasing concentrations of EFG were added to the pre-translocation complex. The reaction took place for 1 min, after which translocation was again titrated by reaction with puromycin.

Statistics

One-way ANOVA was used to estimate the mean values and data variability. The Scheffé F-test was used to determine significant differences between means. All statistical tests were performed using a SPSS program for MS Windows, Release 6.0.

RESULTS

Identification of ABA-spermine cross-linking sites in 23S rRNA

The photoreactive polyamine, ABA-spermine, contains an azidobenzamidino group linked to the N^1 position of spermine. The arylazido tether (ABA-) is ~9 Å long and, therefore, the target site in 23S rRNA is approximately within a distance of one nucleoside from the N^1-amino group of spermine. Activated by ultraviolet light (300 nm), the azido-group reacts immediately with a neighboring group of ribosomes and results in covalent attachment to rRNA or ribosomal proteins, as shown previously (20,34). Following this strategy, we found that >57% of cross-linked photoprobe is preferentially distributed to rRNA. Identification of the cross-linking sites was achieved by primer-extension analysis. We analyzed the entire 23S rRNA, except for nucleosides 2870–2904. In fact, no cross-linking sites occur into this extreme region, as detected by RNase H cleavage experiments (Supplementary Table 1). Representative auto-radiograms obtained by primer-extension analysis are shown in Figures 1 and 2, and the modified nucleosides by ABA-spermine are summarized in a refined secondary structure model of 23S rRNA (Figure 3). Also, a detailed presentation of the 23S rRNA residues labeled under several conditions is given in Supplementary Table 2. The probing data obtained are unavoidably minimal, since some stops cannot be accounted for, due to the co-occurrence of control bands on the auto-radiograms. These may arise from cuts incurred during the treatment of ribosomes and from post-transcriptional modifications or stable structures of rRNA, which cause pausing of reverse transcriptase. As shown in Figure 3, the authentic reverse transcriptase stops are almost

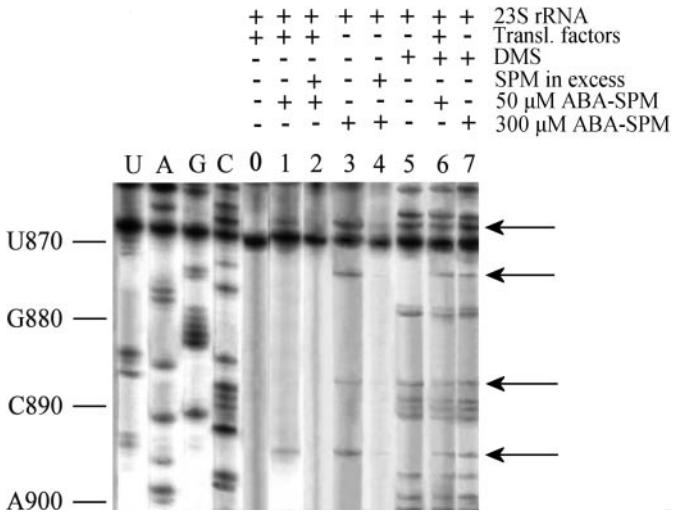

Figure 1. ABA-spermine cross-linking at the tip of helix H38. Naked 23S rRNA was photolabeled with ABA-spermine, and then was monitored by primer-extension analysis. The primer for the reverse transcriptase reaction was complementary to 23S rRNA positions 962–978. U, A, G and C are dideoxy sequencing lanes. Lane 0, control (non-photolabeled sample); lane 1, sample photolabeled with 50 μM ABA-spermine in the presence of translation factors; lane 3, sample photolabeled with 300 μM ABA-spermine in the absence of translation factors; lanes 2 and 4, samples like those used in lanes 1 and 3, respectively, but photolabeled in the simultaneous presence of spermine in excess; lane 5, sample modified by DMS; lanes 6 and 7, samples treated as those in lanes 1 and 3, respectively, and then modified by DMS. The stops of reverse transcriptase reaction due to ABA-spermine cross-linking are indicated by arrows.

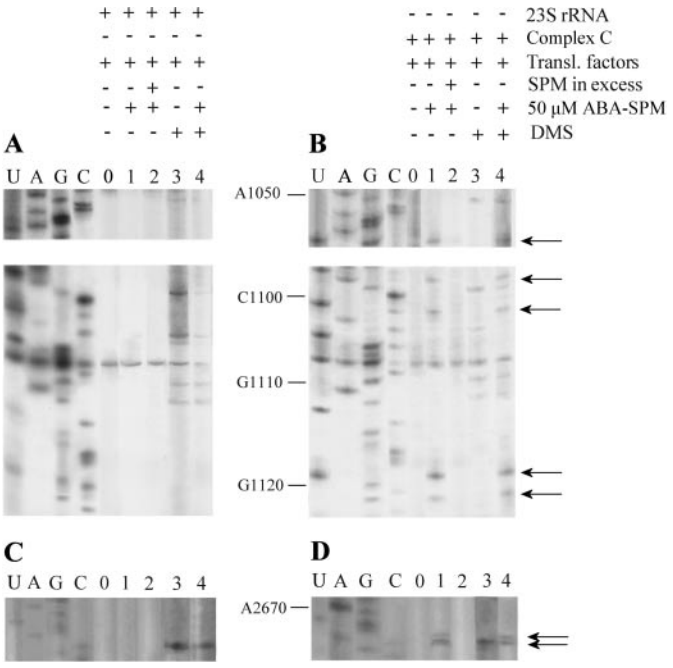

Figure 2. ABA-spermine cross-linking in helices H42–H44 of the GTPase center. (**A** and **C**) Naked 23S rRNA photolabeled with 50 μM ABA-spermine in the presence of translation factors and (**B** and **D**) 23S rRNA isolated from complex C photolabeled under the same conditions were monitored by primer-extension analysis. The primers for the reverse transcriptase reaction were complementary to 23S rRNA positions (A and B) 1157–1173 and (C and D) 2781–2797. U, A, G and C are dideoxy sequencing lanes. Lane 0, control (non-photolabeled sample); lane 1, sample photolabeled with ABA-spermine; lane 2, sample photolabeled with ABA-spermine in the simultaneous presence of spermine in excess; lane 3, sample modified by DMS; lane 4, sample photolabeled with ABA-spermine, and then modified by DMS. The stops of reverse transcriptase reaction due to ABA-spermine cross-linking are indicated by arrows.

always detected as single stops. In some cases, a long stretch of neighboring stops is observed. Frequently, these clusters show a strong 3′ band, as observed for A226–C228. Such a pattern is probably due to 'stuttering' of reverse transcriptase. However, in cases such as in the long stretch of stops observed at positions C1941–U1944, the intensities of the bands suggest that all nucleosides may be modified. To check for non-specific photo-incorporation, control experiments were performed in which natural polyamines in excess were added in the incubation mixture during photolabeling. When spermine was used as competitor, the authentic stops of reverse transcriptase (Figures 1 and 2) were almost eliminated. The competition potency of polyamines fell into the rank spermine > spermidine ≫ putrescine. In fact, at a ratio of 250-fold spermine to photoprobe, labeling of 23S rRNA was reduced by ∼90%, while the same excess of spermidine caused a reduction of <10%. With a few exceptions, including cross-linking at A404, A503, G506 and nucleosides of the 1490–1570 and 1941–1944 regions in 50S subunits and post-translocation ribosomes, the cross-linking pattern for the remaining labeling was not essentially altered. Competition experiments with polyamines at higher concentrations could not be performed, because ribosomes were precipitated at such concentrations. Monovalent ions, such as Na^+ or NH_4^+, did not compete, even at high concentrations needed to compensate for their lower charge density. By increasing the concentration of Mg^{2+}, the labeling of 23S rRNA decreased in a dose-dependent manner up to 50 mM Mg^{2+}, and then remained constant (∼60% of the initial labeling). At 10 mM Mg^{2+}, a 12% reduction in photolabeling was recorded. In previous studies [(29) and references therein], it has been noted that high concentrations of competitors are required to affect photoaffinity labeling; ionic competitors, such as natural polyamines, would be expected to antagonize the irreversible binding of the photoprobe during the initial recognition phase but not once covalent binding has occurred.

As shown in Figure 3, both helices and single-stranded regions are susceptible to cross-linking, with non-paired nucleosides being slightly preferable (65%). It is evident that the cross-linking pattern depends on the photoprobe concentration. For instance, the domains primarily labeled by 50 μM ABA-spermine in naked 23S rRNA are I, II and V. Increase of photoprobe concentration to 300 μM results in enrichment of the cross-linking pattern by additional sites belonging to domains I–V. From Figure 3, it is also evident that another factor which influences the number and intensity of the autoradiography bands is whether 23S rRNA is photolabeled naked or in complex with ribosomal proteins, poly(U) and tRNAs. Assembly of 50S ribosomal subunit favors 23S rRNA interactions with ABA-spermine, except for nucleosides localized at the tip of helix H38. Finally, association of 30S with 50S ribosomal subunits, poly(U) and AcPhe-tRNA further alters the susceptibility of 23S rRNA for ABA-spermine cross-linking, particularly to helices H11–H13, H21, H63, H80, H84, H90 and H97. No prominent changes in the cross-linking pattern are observed when translation factors are

included in the irradiation buffer, except in rare cases, such as in loop-1095, the region around position 1942, helix H80 and the central loop of domain V. Nevertheless, from a functional point of view, the importance of these rare changes is beyond doubt.

Chemical probing experiments indicated that assembly of the 50S ribosomal subunit results in protection of several regions in 23S rRNA. Both association of ribosomal subunits and binding of AcPhe-tRNA decrease further the reactivity of 23S rRNA. Namely, nucleosides located at the tips of H34 and

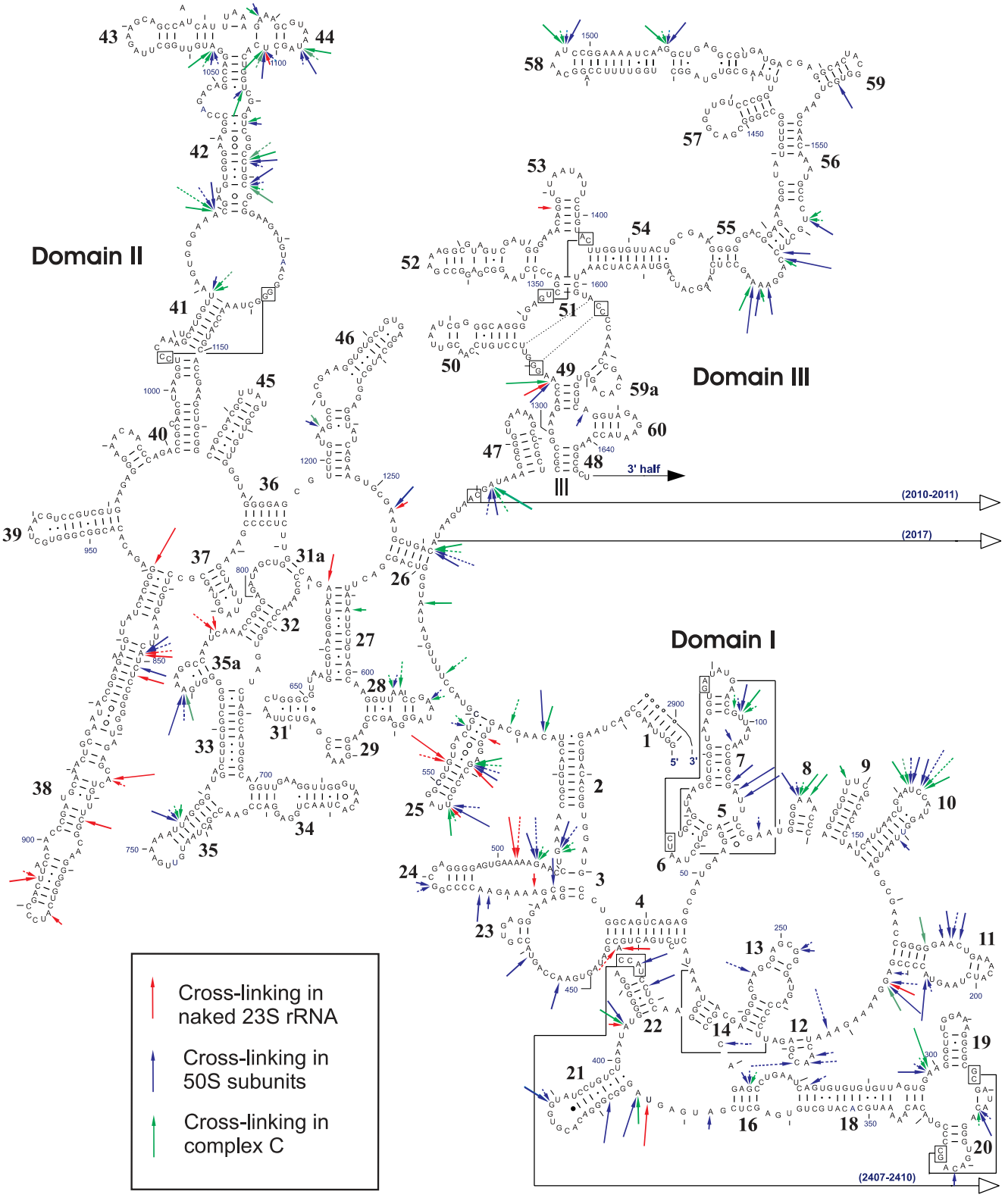

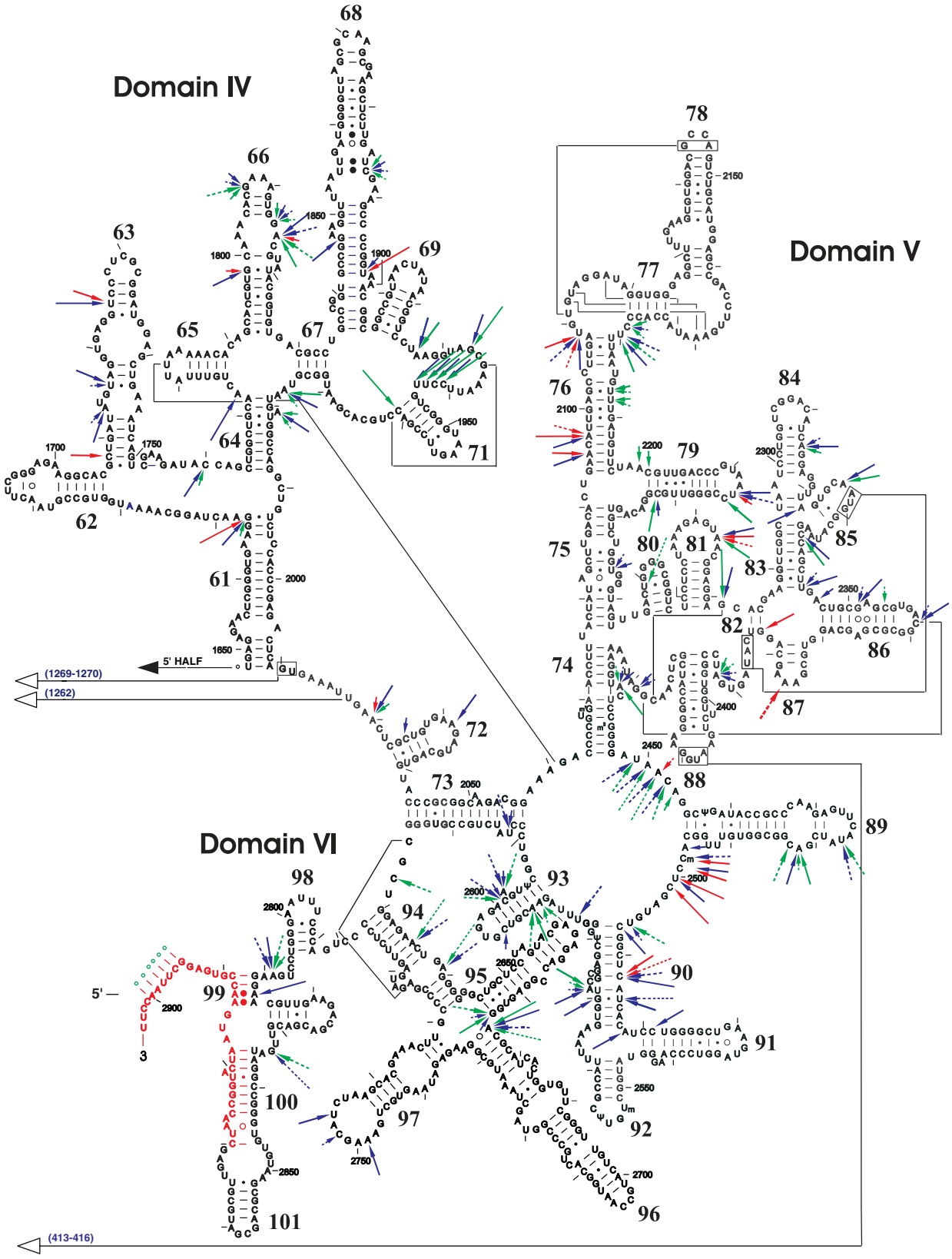

Figure 3. Secondary structure diagram showing the ABA-spermine cross-linking sites in 23S rRNA of *E.coli*. Cross-links of ABA-spermine are marked with red (cross-linking in naked 23S rRNA), blue (cross-linking in 50S subunit) and green arrows (cross-linking in complex C) in a secondary structure model of 23S rRNA from *E.coli* (cited at http://www.rna.icmb.utexas.edu). The arrows, solid or discontinuous, indicate sites labeled with 300 μM ABA-spermine in the absence of translation factors (condition A) or with 50 μM ABA-spermine in the presence of translation factors (condition B), respectively. Long arrows, strong cross-links; medium arrows, intermediate cross-links; short arrows, weak cross-links. Nucleosides not analyzed are shown in red.

H38, in helices H63, H69–H71, H81, H84, H97, and especially A2451 in the central loop of domain V, are protected against DMS. In contrast, nucleosides A1866, A1891, A1896, A2602 C2214 and A2392 become more reactive. These results are consistent with previous studies (1,39–41) and certify to the correct folding of our ribosomes. Beyond these observations, we found that cross-linking of ABA-spermine causes further alterations in the reactivity of 23S rRNA toward DMS, in a manner depending on the photoprobe concentration and the status of 23S rRNA. The results of these experiments are summarized in Table 1. Although alterations in reactivity toward DMS suggest conformational rearrangements in ribosomal structure, no detectable changes in the sedimentation profile of 50S ribosomal subunits or complex C were observed.

Effect of photolabeling on the binding of Ac[^{3}H]Phe-tRNA to the P- and A-sites of poly(U)-programmed ribosome

Poly(U)-programmed ribosomes, photolabeled as a whole or reconstituted from photolabeled 50S subunits and intact 30S subunits, were assayed for their efficiency to bind AcPhe-tRNA. As shown in Table 2, when totally photolabeled ribosomes are used, the binding to both P- and A-sites is much higher, compared with that obtained by native ribosomes. In contrast, cross-linking of ABA-spermine to 50S subunits has only a slight effect on the binding properties of hybrid poly(U)-programmed 70S ribosomes reconstituted from photolabeled 50S subunits and intact 30S subunits. To check whether this deviating behavior may be due to some inability of photolabeled 50S subunits to associate, spermine-treated 50S subunits were incubated with native 30 subunits in a molar ratio of 1:2 under conditions promoting their association. Next, the formation of 70S ribosomes was monitored by sucrose gradient sedimentation. These tests clearly demonstrated that >85% of photolabeled 50S subunits are competent for association with 30S subunits (data not shown) and that the peak of the hybrid 70S ribosomes co-sediments with that of native 70S ribosomes.

Effect of photolabeling on PTase activity

In agreement with previous results (34), we found that photolabeling of complex C with ABA-spermine does not remarkably change the extent of peptide bond formation when translation factors are included in the irradiation mixture (Table 3). However, sizeable enhancement in the extent is recorded when ABA-spermine cross-links either to whole complex C or to its 50 subunit in the absence of translation factors. Moreover, photo-incorporation of ABA-spermine into whole complex C or its 50S subunit increases k_3, without affecting the K_s value. This is true when photolabeling is carried out under condition B (50 μM ABA-spermine plus translation factors). In contrast, photolabeling under condition A (300 μM ABA-spermine minus translation factors) results in a complex C, which is less active than the control. Control experiments also indicated that pre-labeling of translation factors or poly(U) with ABA-spermine has no effect on the catalytic properties of the reconstituted complex C. Interestingly, ribosomes reconstituted from photolabeled 23S rRNA and native 5S rRNA, TP50 and 30S subunits are completely

Table 1. DMS modification data obtained from naked 23S rRNA, 50S ribosomal subunits and complex C photolabeled with 300 μM ABA-spermine in the absence of translation factors (condition A) or with 50 μM ABA-spermine in the presence of translation factors (condition B)[a]

Domains of 23S rRNA	Target molecule Naked 23S rRNA A	B	50S ribosomal subunit A	B	Complex C A	B
I	(A160), (A161), (C163)–(A165), (A167), (A226), (C240), (A241), (A244), (C264), (A278), (A279), (A428)–(A430), **A501**, **A502**, (A505), (A547), (A556)	**A190–C192**, **A299**, **A300**, **A340**, **A182**, **C183**, **A501**, **A502**, **A404**, **A412–C414**, **A428–A430**	**A161**, **C164**, **A165**, **A340**	(A507), (A526)–(A529), (A547), (A556), **A374**, **C383–C385**, **A391**, **A412–C414**, **C164**, **A165**, **A167**		(A412)–(A415)
II	(A845), (C888), (C889), (A910), (A911), **A764**, **A781–A783**, **A789**, **A792**, **A793**, **A1126**, **A1127**, **A1129**, **A1133**, **A1175**, **A1265**, **A1268**, **A1269**	(A845), **A789**, (A886), (C888), (C889), (A1048), (A1089), (A1095), (A1096), (A1098), (A1103), (A1126), (A1127), (A1129), (A1133), (A1175), **A1265**, **A1268**, **A1269**	(A910), (A911), (A1048), (A1089), (A1095), (A1096), (A1098), (A1103)	**C876–A878**, (A910), (A911), (A1098), (A1103), (A1265), (A1268)	**A829**, **A845**, **C876–A878**, (A1048), (A1089), (A1095), (A1098), (A1103)	(A941), (A943)–(A945), (A1095), (A1096), (A1098), (A1265), (A1268), (A1272)
III	(A1321), (A1322), (A1365)–(A1367), (A1378), (A1392), (A1395), **A1420**, **A1427**, **A1566**, **A1683**, **A1972**	(A1321), (A1322), (A1353), (A1373), (A1378), (A1392), (A1393), (A1395), **A1972**		**A1494**, **A1496**, (A1972)		(A1972)
IV		**A1966**		**A1966–A1969**		**A2013**, **A2014**
V	(A2285), (A2376), **C2467–A2469**, **C2475**, **A2476**, **A2478**, **A2482**, **C2483**, **A2497**	(C2501)	(A2114), (A2117), (A2119), (C2306), (A2309)–(A2311), (A2376)–(A2378), **A2478**, **C2483**, **A2598**	(A2376)–(A2378), (A2388), **A1936–A1938**, **C1941**, **C1942**, **A1966**, **C1967**, **A1969**, **A2058**, **A2059**, **A2082**	**A2058**, (A2376)–(A2378)	**A2013–A2015**, **A2019–C2021**, (A2376)–(A2378), (A2388), **A2497**, **C2573**, **A2598**
VI	**A2660**, **A2662**, **A2667**, **A2681**, **A2682**		(A2748)–(A2750), (C2858), (A2860)	**C2681**, **A2682**, **C2712**, **A2721**, **A2726**		**C2681**, **A2682**, **A2721**, **A2726**

[a]Nucleosides exhibiting increased reactivity, compared with the control (non-labeled sample), are indicated in bold, while nucleosides with decreased reactivity are shown in parenthesis.

inactive toward puromycin, although they exhibit a normal sedimentation profile.

Effect of photolabeling on translocation

Translocation was titrated with a mixture of 2 mM puromycin and 5 μM thiostrepton for 3 min at 25°C. In agreement with previous reports (42,43), we found that thiostrepton at 5 μM, while preventing translocation during the titration process, does not affect the puromycin reaction.

To test whether ABA-spermine photo-incorporation could interfere with translocation of AcPhe-tRNA from the A-site to the P-site of poly(U)-programmed ribosomes, two series of experiments were carried out. In the first, translocation was studied in buffer A containing 0.12 mM GTP and spermine at final concentrations ranging from 0 to 300 μM, i.e. under conditions allowing reversible interaction between ribosomes and the polyamine. As shown in Figure 4A, EFG at 0.015 μM promotes rapid translocation that is almost complete within 30 s, regardless of whether spermine is present or absent. However, in the absence of EFG, translocation is slower

Table 2. Effect of ABA-spermine cross-linking in 23S rRNA on AcPhe-tRNA binding to poly(U)-programmed ribosomes[a]

Ribosomal species	ABA-spermine concentration (μM)	P-site bound AcPhe-tRNA per 70S ribosome	A-site bound AcPhe-tRNA per 70S ribosome
Unlabeled		0.067 ± 0.005	0.041 ± 0.003
Labeled in	50	0.072 ± 0.004	0.042 ± 0.003
50S subunit	300	0.109 ± 0.007	0.052 ± 0.006
Totally labeled	50	0.148 ± 0.011	0.092 ± 0.007
	300	0.345 ± 0.025	0.153 ± 0.011
Labeled in 23S rRNA	50	n.d.[b]	0.040 ± 0.003

[a]The binding mixture (25 μl) contained 50 μM HEPES-KOH, pH 7.2, 6 mM magnesium acetate, 100 mM NH_4Cl, 0.4 mM GTP, 8 μg poly(U), 5.3 pmol Ac[^{3}H]Phe-tRNA, 6 mM 2-mercaptoethanol and 10.4 pmol 70S ribosomes untreated or photolabeled with ABA-spermine, and pre-filled (A-site binding) or not pre-filled (total binding) in their P-site by $tRNA^{Phe}$. The reaction was carried out for up to 30 min at 25°C. The maximal level of binding was measured by nitrocellulose filtration. The P-site bound Ac[^{3}H]Phe-tRNA was estimated from the total binding by titration with puromycin (2 mM, 10 min at 25°C). Ac[^{3}H]Phe-tRNA values are expressed as means ± SD ($n = 5$).
[b]Although the total binding was 0.100 Ac[^{3}H]Phe-tRNA residues per ribosome, P-site binding could not be determined (n.d.), because the reconstituted ribosomes were inactive in PTase.

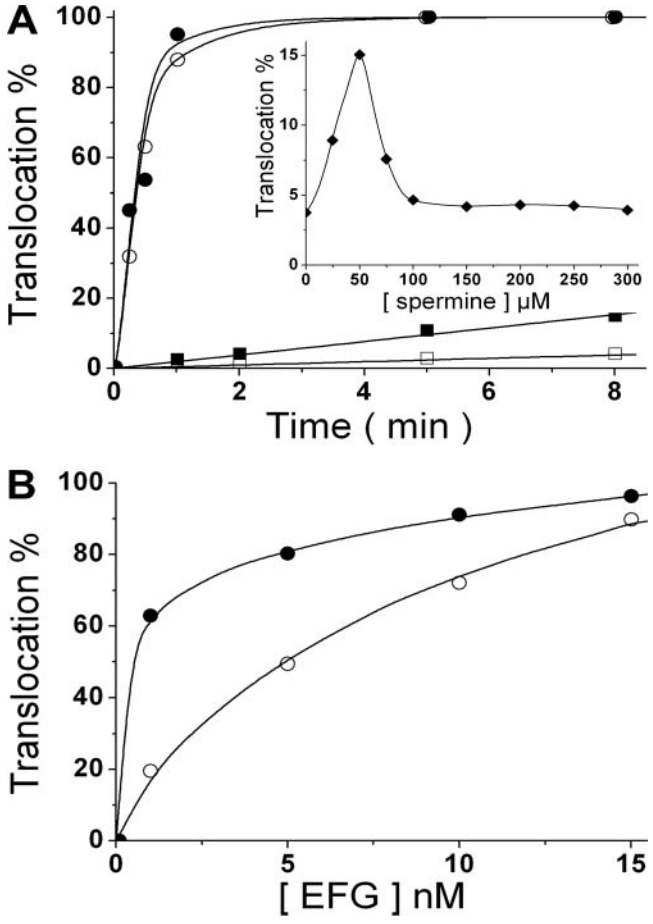

Figure 4. Influence of spermine on spontaneous and enzymatic translocation. (**A**) Time course of (circles) enzymatic and (squares) spontaneous translocation. Aliquots of pre-translocation complex, i.e. poly(U)-programmed 70S ribosomes occupied at the P- and A-sites with $tRNA^{Phe}$ and Ac[^{3}H]Phe-tRNA, respectively, were incubated for the indicated time intervals in buffer A containing 0.12 mM GTP, (open symbols) in the absence or (filled symbols) in the presence of 50 μM spermine. Enzymatic translocation was obtained by the addition of 15 nM EFG in the incubation mixture. Inset, dependence of spontaneous translocation on spermine concentration. To a fixed amount of pre-translocation complex, increasing concentrations of spermine were added and translocation was allowed to proceed for 10 min at 25°C. (**B**) Dependence of translocation on EFG concentration. Pre-translocation complex was incubated with different amounts of EFG for 1 min at 25°C (open circles) in the absence or (filled circles) in the presence of 50 μM spermine. In all drawings, translocation of 100% represents conversion of all ribosomes at the pre-translocation state into the post state.

Table 3. Extent and kinetic parameters of AcPhe-puromycin synthesis carried out with complex C totally or partially labeled by ABA-spermine[a]

Complex C species	Translation factors	Photoprobe concentration (μM)	Extent of AcPhe-Puromycin synthesis (%)	k_3 (min^{-1})	K_s (μM)
Unlabeled	−	0	32	1.52 ± 0.05	625 ± 31
	+	0	79	2.22 ± 0.06	615 ± 18
Totally labeled	−	300	81	1.15 ± 0.04	625 ± 30
	+	50	86	3.46 ± 0.03	635 ± 32
Labeled in 50S subunit	−	300	55	1.55 ± 0.05	635 ± 31
	+	50	83	3.07 ± 0.05	615 ± 31
Labeled in 23S rRNA	−	50	1	n.d.	n.d.

[a]Each species of complex C reacted with puromycin in buffer containing 6 mM Mg^{2+} and 100 mM NH_4^+. K_s and k_3 values were determined by non-linear regression fitting of k_{obs} and [S] values into Equation 2. Extent values are expressed as the percentage of radioactive Ac[^{3}H]Phe-tRNA added into the reaction mixture. K_s and k_3 values are given in means ± SD ($n = 5$).

and proceeds in a time- and spermine-dependent manner. The optimum concentration of spermine was found to be 50 μM (Figure 4A, inset). To examine the effect of spermine on EFG requirements for efficient translocation, increasing concentrations of EFG were added to a fixed amount of pre-translocation complex in buffer A containing or non-containing 50 μM spermine, and translocation was allowed to proceed for 1 min at 25°C. As shown in Figure 4B, the extent of translocation in both cases increases with EFG concentration and reaches a plateau. Nevertheless, the concentrations of EFG at which 50% translocation is achieved are 0.58 and 5 nM, respectively. These results show that ribosomes are more efficient in enzymatic translocation in the presence of polyamines than in their absence.

In the second series of experiments, pre-translocation complexes unlabeled, totally labeled or labeled by ABA-spermine in each one of their subunits were assayed for their translocation efficiency in buffer A. Spontaneous translocation was found again to proceed slowly and in a linear fashion at least up to 8 min. As indicated in Figure 5A, pre-translocation complex totally labeled or partially modified in its 50S subunit by ABA-spermine is more efficient in translocation compared with untreated complex or complex labeled only in its 30S subunit. Furthermore, photolabeling of the whole ribosomal complex or of its 50S subunit has a sparing effect on EFG requirements (Figure 5B). The whole set of data supports the notion that ribosomes bearing polyamines, especially in their 50S subunits, are more efficient with regards to spontaneous and enzymatic translocation than control ribosomes. Interestingly, ribosomes reconstituted from 30S subunits, 5S rRNA, TP50 and photolabeled 23S rRNA were found to be defective in translocation. However, it should be noticed that naked 23S rRNA never exists as a separate entity in the cytoplasm, so that even a careful 'renaturing' incubation of the isolated 23S rRNA prior to photolabeling may be not very meaningful. If so, ABA-spermine probably stabilizes an artificial conformation in naked 23S rRNA, so that ribosomes reconstituted from 23S rRNA modified in this way are not functional. Supportive evidence is provided by the different photolabeling and DMS-protection patterns observed between naked and assembled 23S rRNA with ribosomal proteins and AcPhe-tRNA.

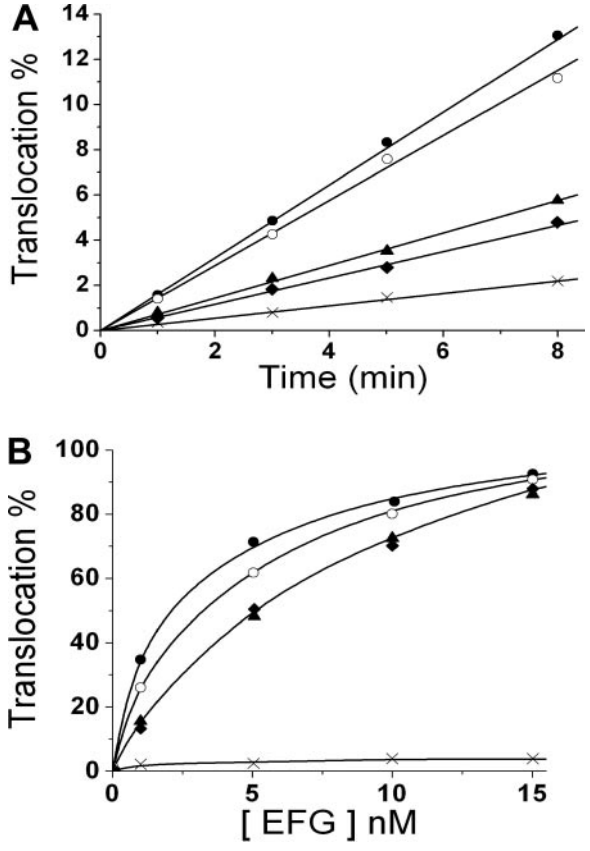

Figure 5. Effect of ABA-spermine cross-linking to ribosomes on translocation. (**A**) Time course of spontaneous translocation. Aliquots of pre-translocation complex, i.e. poly(U)-programmed 70S ribosomes occupied at the P- and A-sites with $tRNA^{Phe}$ and Ac[^{3}H]Phe-tRNA, respectively, were incubated for the indicated time intervals in buffer A containing 0.12 mM GTP in the absence of free spermine. The pre-translocation complex used was (filled diamonds) unlabeled, (filled circles) totally labeled or labeled in its (open circles) 50S subunit, (filled triangles) 30S subunit, or (crosses) 23S rRNA by 50 μM spermine. (**B**) Dependence of translocation on EFG concentration. The symbols are the same as those used in (A).

DISCUSSION

In the present work, *E.coli* 23S rRNA was labeled with a photoreactive polyamine, ABA-spermine. This approach has led to a map of spermine binding sites in 23S rRNA, which reveals new features that start to 'make sense' in terms of explaining the effects of polyamines on the structure and function of the large ribosomal subunit. It should be mentioned here that an optimized poly(Phe) synthesizing *in vitro* system, from *E.coli* cells with a rate and accuracy close to the corresponding *in vivo* studies, requires both spermine and spermidine (25). However, in a recent study, we found that the use of the above optimized polyamine buffer instead of spermine alone does not significantly change the kinetic features of puromycin reaction and the ability of ribosomes to interact with several antibiotics (22). The advantages of the used photoaffinity labeling technique over other approaches have been previously discussed in detail (34).

The number of cross-linking sites determined in the present work is higher than that calculated by Hill-plot analysis in a previous study (20). However, this contradiction may be more apparent than real, since adjacent nucleosides in the primary, secondary or tertiary structure of 23S rRNA may represent the same binding site. The nucleosides labeled by ABA-spermine are dispersed over a considerable length of the 23S rRNA but, notably, the cross-linking pattern depends on the status of 23S rRNA (naked, assembled in 50S subunit or in complex C), the concentration of photoprobe and the presence of translation factors. Furthermore, there is a discrepancy between divalent-metal-ion binding sites (11–13,16) and the sites we propose here, although there are areas of agreement. This observation confirms previous suggestions that structural and functional ribosomal alterations caused by polyamines may be different from those induced by divalent metal ions (8,44).

Two different modes of polyamine binding to nucleic acids have so far been proposed (11,45): non-specific binding concerning polyamines diffusing freely within a prescribed volume around the nucleic acid molecule, and site-specific

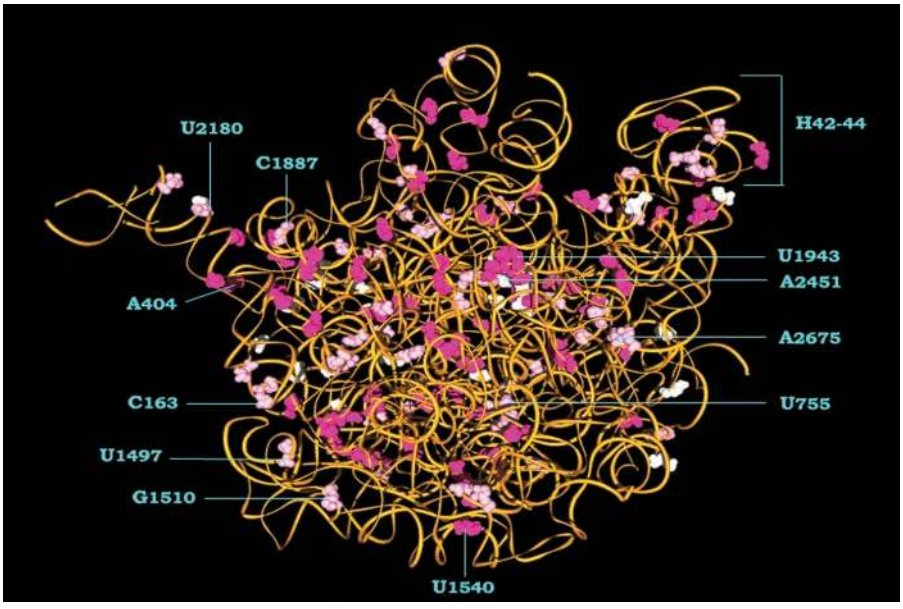

Figure 6. Three-dimensional representation showing the ABA-spermine cross-linking sites in 23S rRNA. The cross-linking data are superimposed on a tertiary structure model of the eubacterium *D.radiodurans* 23S rRNA (48) generated by using the Swiss-PdbViewer. The labeled nucleosides (*E.coli* numbering) are shown with red (found only under condition B), white (found only under condition A) or pink spheres (found under both conditions).

binding occurring in defined electro-negative binding pockets via direct bonding with nucleic acid residues. Tandem G•U wobble pairs or G•C pairs followed by non-canonical base pairs (U•U or G•A) have been previously found in such cation-binding motifs of rRNA (16,46,47). In the present study, we observed that the primarily labeled nucleosides in single-stranded regions are A and U (75%). In contrast, the cross-linking sites in double-stranded regions are distributed more equally among the four nucleosides. Nevertheless, a slight preference for C and U residues (60%) is detectable. As indicated by competition experiments using natural polyamines and metal ions as competitors, most of the cross-linking sites appear to be specific. The remaining sites are located in regions accessible to cleaving metal ions or/and belong to regions exposed to cytosol. For instance, the sensitivity of H70 against ABA-spermine survives the competition effect of spermine, while it is strongly reduced by Mg^{2+} ions. It is relevant that the same region in *E.coli* ribosomes is cleaved by Ca^{2+} and Eu^{3+} ions (11,12), while in *H.marismortui* it forms outer sphere contacts with Mg^{2+} ions (16). On the other hand, when the cross-linking data are superimposed on a tertiary structure model of the eubacterium *Deinococcus radiodurans* 23S rRNA (48), it becomes clear that certain cross-links in domains I (U99, G110, A222, A299, C331, A404, C418, A483, A503, G506, G539 and U545), II (A849, C851 and A1205), III (region 1490–1570) and VI (A2809 and G2834) are situated on the cytosolic surface of the large ribosomal subunit (Figure 6). Some of these sites are also in close proximity with positions accessible to cleaving metal ions (11,12). Therefore, it is tempting to suppose that cross-linking within these regions concerns non-specifically bound polyamines. Independent of the specificity, polyamine binding to certain regions may be beneficial for the stabilization of the tertiary structure. Noteworthy is the binding to C1261 and A1272. These nucleosides flank the sequence 1262–1270, an element of domain II that interacts with 2010–2017 to form an irregular helix in the core of 23S rRNA. In fact, this sequence comprises a loop-E motif; disruption of either base pair flanking the motif has been shown to impair the ability of ribosomes to engage in protein synthesis (49). Cross-links are also observed in four-helix junctions or helices containing non-canonical base pairs. For instance, polyamine binding to A1977 in 50S subunits or complex C may play a direct role in the organization of this junction, while binding at the neighboring bulged base A1981 is most probably related to stabilization of the two adjacently situated G•U wobble pairs. Also, cross-linking to G2383 is most likely related with the stabilization of a four-helix (H82, H83, H86 and H87) junction in naked 23S rRNA. Assembly of ribosomal proteins in 50S subunits or in complex C causes tightened folding in this region as indicated by DMS-protection experiments, which probably compels polyamines to bind other sites, such as U2344 and A2346, located around this junction.

Compared with that found in naked 23S rRNA, the 50S subunit cross-linking pattern is enriched by additional accessible sites to ABA-spermine. In domain I, most of these sites coincide or are adjacent to 23S rRNA residues that contact proteins L4 and L24. It is known that both proteins attached to domain I play a crucial role in the local conformation and ribosomal assembly (50). Therefore, it is reasonable to suggest that, apart of the role of ribosomal proteins, polyamines may also influence the conformation of domain I. Further evidence that supports this notion is provided by DMS-protection experiments, indicating that photolabeling of 50S subunits causes diverse changes in the tertiary structure of domain I. Other examples of cross-linking, which may be implicated in protein binding, are related with domain V labeling. U2180 is located within a loop interconnecting H76 and H78. It has been postulated that this loop may play a critical role in the formation of an Mg^{2+} binding site involved in the binding of protein

L1 (14). Thus, attachment of polyamines within this region may contribute to the binding of L1 and the organization of the local conformation. Nevertheless, metal ions in the L1 binding region of 23S rRNA were not detected in the current electron density map for the large subunit of *H.marismortui* (16), a fact which makes the above postulated role of Mg^{2+} and polyamines questionable. Other cross-linking sites probably related with protein binding are G2282, U2477 and C2752. Nucleoside G2282 is noticeably labeled under condition A, whereas U2477 and C2752 are labeled under condition B. These sites are implicated in the binding of L27, L6 and L3, respectively. Interestingly, these proteins are preferentially targeted by ABA-spermine under the same conditions (20).

Complex C was found to be less susceptible to ABA-spermine cross-linking than 50S subunits. Several of the protected sites, such as the tips of helices H84 and H97, and helix H63, are situated on the subunit interface. Therefore, it is reasonable to suggest that their insensitivity to photolabeling may arise from hindering effects caused by subunit association. This is not entirely surprising since DMS probing experiments indicate that regions 1689–1732, 2306–2310 and 2748–2757 are protected upon subunit association, a finding consistent with previous studies (40,41). Noteworthy is the behavior of H38 tip against photolabeling. Cross-linking of ABA-spermine within this region occurs only in naked 23S rRNA. The protection observed in 50S subunits and complex C can be explained by the fact that in isolated 50S subunits the tip of H38 contacts the central protuberance, while in 70S ribosomes participates in bridge B1a which connects the large subunit with the head of the 30S subunit (3). Nevertheless, some regions of the subunit interface seem to escape protection. For instance, C163 is susceptible to ABA-spermine cross-linking either in 50S subunits or complex C. This position has already been found in *H.marismortui* to participate in a cation binding pocket (16), while other crystallographic studies implicate C163 in the structure and properties of bridge B7β postulated to serve as a relay between tRNA interactions in the small subunit and the catalytic center in the large subunit (3). H70 is another example of region preserving its reactivity against ABA-spermine in complex C. H70 lies at the top edge of the PTase cleft and is essential for subunit association and other ribosomal functions (41). Incorporation of so many ABA-spermine molecules into this region reduces its flexibility, a fact that should negatively affect its functions. Indeed, we found that photo-incorporation of ABA-spermine into helix H70 is achieved only when photolabeling is performed in the absence of translation factors and at high concentrations of photoprobe, both conditions reducing ribosomal efficiency for subunit association (20) and catalysis of peptide bond formation (Table 3).

Kinetic experiments show that ribosomes are more efficient in spontaneous or enzymatic translocation when spermine is present than when it is absent (Figures 4 and 5). Consistently, helices H42–H44 involved in the factor-dependent GTPase activity [reviewed in (51)] and the binding of EFG (52) contain weak as well as strong cross-linking sites. Previous studies have demonstrated that NH_4^+ and Mg^{2+} ions bind within this region and stabilize functional tertiary structures [reviewed in (9)]. Therefore, it is tempting to suggest that binding of polyamines may give an extra stability to this region, which may be beneficial to the translocation of tRNAs. Supporting evidence is provided by DMS-protection experiments, indicating that helices H42–H44 in complex C achieve a tighter structure upon ABA-spermine photo-incorporation. Another observation that can explain the effect of polyamines on tRNA translocation is related with the labeling of A2602 and U2584 residues in the central loop of domain V. Next to U2584 is U2585, which along with A2602 bulge into the PTase center, close to the symmetry axis of the catalytic cavity (3,6,53). Both U2585 and A2602 have been envisaged to play a dynamic role in the passage of the tRNA-3′ end from the A- to the P-site; A2602 has been proposed to propel, in concert with the tip of helix H69, the rotatory motion of the tRNA-3′ end, while U2585 has been suggested to anchor the rotatory motion by direct interaction with the tRNA-bound amino acid and assure the proper positioning of P-site substrates (53). Also, strong cross-linking of ABA-spermine occurs into the tip and the internal loop of H89, a helix previously detected to interact with EFG (52), the L7/L12 stalk (54) and 5S rRNA (55).

Interestingly, several cross-links are identified in regions that are important for tRNA binding, a fact supporting the possibility that polyamines may influence the positioning of translation substrates. Nucleosides A191, G248, G389, A454, U459, A482, A483, G489, G506, U2213 and U2613, labeled by ABA-spermine, are located near positions implicated in the P- and E-site binding of tRNA-OP, a $tRNA^{Phe}$ conjugated at various positions with 1,10-phenanthroline (56). Except for cross-linking to G506 that probably participates in a strong cation-binding pocket (11), photo-incorporation into the latter sites is fully eliminated in complex C. This may be due to shielding effects caused by complex C-bound ligands (P-site bound AcPhe-tRNA and E-site bound $tRNA^{Phe}$). Similarly, cross-linking in the tip of helix H38, occurring when photolabeling is applied to naked 23S rRNA, is substantially reduced when 50S subunits or complex C are targeted. H38 is called 'A-site finger', because nucleosides 881–883 contact the D-loop and 898–899 the T-loop of A-site bound tRNA (3). The insensitivity of the H38 tip to ABA-spermine during 50S subunit or complex C photolabeling is consistent with the observation that 50S subunit photolabeling fails to affect AcPhe-tRNA binding to the A-site (Table 2). In contrast, photolabeling of the whole complex C is beneficial. However, under the latter condition, 30S subunit and AcPhe-tRNA are also targeted by ABA-spermine, a fact that favors tRNA binding (34). Nevertheless, some nucleosides implicated in tRNA binding preserve their reactivity against ABA-spermine even in complex C. For instance, nucleoside C1887 is targeted by ABA-spermine upon any ionic condition, either in 50S subunits or in complex C. Nucleoside C1887 is located within a pocket created by two non-canonical base pairs in the vicinity of residue C1892. X-ray crystallography has detected a minor groove interaction between C1892 and position 71 of E-site bound tRNA (3). It seems likely that polyamines attached to this site may facilitate the positioning of E-site bound tRNA. Also, noteworthy are two strong cross-links observed exclusively in complex C; the first position, U2249, is situated on helix H80, while the second, A2590, is positioned in H93. Nucleoside U2249 forms a wobble base pair with G2255 allowing the N^2 amino-group of guanine to be reactive against ABA-spermine. This wobble base pair is situated adjacently to the P-loop (G2251–G2253) that contacts nucleoside C74

of P-site bound tRNA (1). On the other hand, helix H93 is squeezed between the respective CCA ends of A- and P-site bound tRNAs (3). Interestingly, both U2249 and A2590 become insensitive to cross-linking under condition A. Therefore, it is tempting to suggest that binding of polyamines to those regions under condition B facilitates the accommodation of AcPhe-tRNA aminoacyl-end to the P-site of the catalytic cavity. In contrast, both the insensitivity of A-loop (tip of helix H92) to photolabeling and the stability of K_s value under any experimental condition suggest that a similar effect of polyamines on the positioning of aminoacyl-end to the A-site must be excluded.

The significance of the central loop of domain V in PTase activity is beyond doubt. Therefore, the finding that cross-linking sites of ABA-spermine are identified within this loop is of particular merit. Under condition A, the nucleosides primarily labeled in 50S subunits are A2497, C2499, U2500 and C2507. Under condition B, photo-incorporation is preferentially directed to U2449–C2452, C_m2498, U2506, U2584, C2601 and A2602. Crystallographic studies have localized A2451 at the bottom of the catalytic cavity on the opposite side of A2602 (3). Mutations at A2451 reduce the activity of ribosomes for transpeptidation and peptidyl-tRNA hydrolysis to about one-half of the activity of native ribosomes (57). Similar properties are also exhibited by U2506, a nucleoside situated 9 Å from A2451. Nucleoside A2451 was proposed by Nissen *et al*. (6) as a catalytic 23S rRNA residue involved along with G2447 and A2450 in a charge relay system, in which a potassium ion also participates. At first glance, this is in agreement with isotope exchange experiments and studies regarding the pH dependence of peptide-bond formation. However, the proposed model of catalysis was reconsidered later by several studies supporting a role for A2451 in positioning the substrates (physical catalysis) and/or water exclusion rather than in a direct participation in chemical catalysis (2,51,58). Such a role satisfies the involvement of this region in the binding of PTase substrates and antibiotics (1,3,51,59). Finally, mutations at U2585 and A2602 cause lethal growth phenotypes in *E.coli*, by severely decreasing peptide release over transpeptidation. (57). Consistently, nucleosides around U2585 and A2602 are cleaved by release factors tethered with Fe^{2+}-BABE (60–62) and are targeted by inhibitors of PTase (51,53,59,63). Given that photo-incorporation of ABA-spermine into 50S subunits under condition B improves the PTase activity, it is reasonable to assume that attachment of polyamines to the nucleosides mentioned has a beneficial effect on this function. Since the terminal amino groups of spermine have a neutral pK, this polyamine may provide the active center with a group that serves as a stabilizer of intermediates or as a general acid/base during peptide bond formation. Nevertheless, the prevailing evidence that ribosome performs its catalytic task by physical catalysis rather than by participating in actual chemical events prompts us to suggest that the main contribution of polyamines on PTase activity is the provision of a frame for precise positioning of the P-site tRNA substrate.

In conclusion, it is striking that most of the identified polyamine binding sites *in vitro* are related with ribosomal regions involved in prominent ribosomal functions, including positioning and translocation of tRNA substrates, binding of ribosomal factors and antibiotics, subunit association and activity of PTase. Spermine is the parent compound of a large number of synthetic polyamine analogs with antitumor activity (26). Extensive biochemical studies have focused on the mechanism by which these compounds act *in vivo*. On the other hand, several studies have detected that the tertiary structure of ribosomes is conserved in all living organisms, a fact supporting the notion that conclusions emerging from studies in eubacteria may extend to cells of higher organisms. Consequently, our studies on the role of spermine on protein synthesis could be of interest to other investigators working on the design of new synthetic analogs of spermine with antitumor activity. Nevertheless, in the absence of exact knowledge regarding the ribosome interaction with polyamines in the context of a cell, everyone must be careful with interpreting the role of polyamines in the ribosome structure and function. Current work in our laboratory focuses on the interaction of spermine with the second rRNA constituent of the large ribosomal subunit, 5S rRNA, based on the prediction of the present study that such interactions may actually occur.

ACKNOWLEDGEMENTS

The authors thank Dennis Synetos for critical reading of the manuscript, as well as Spyridoula Agelakopoulou and Elsa Kalpaxis for technical assistance. The authors also thank European Social Fund (ESF), Operational Program for Educational and Vocational Training II (EPEAK II), and particularly the program IRAKLEITOS, for funding the above work. A.D.P. would like to thank the Research Committee of the University of Patras (Programme K. Karatheodori) for support. Funding to pay the Open Access publication charges for this article was provided by the University of Patras.

Conflict of interest statement. None declared.

REFERENCES

1. Green,E. and Noller,H.F. (1997) Ribosomes and translation. *Annu. Rev. Biochem.*, **66**, 679–716.
2. Ramakrishnan,V. (2002) Ribosome structure and the mechanism of translation. *Cell*, **108**, 557–572.
3. Yusupov,M.M., Yusupova,G.Z., Baucom,A., Lieberman,K., Earnest,T.N., Cate,J.H.D. and Noller,H.F. (2001) Crystal structure of the ribosome at 5.5 Å resolution. *Science*, **292**, 883–896.
4. Moore,P.B. and Steitz,T.A. (2002) The involvement of RNA in ribosome function. *Nature*, **418**, 229–235.
5. Noller,H.F., Hoffarth,V. and Zimniak,L. (1992) Unusual resistance of peptidyl transferase to protein extraction procedures. *Science*, **256**, 1416–1419.
6. Nissen,P., Hansen,J., Ban,N., Moore,P.B. and Steitz,T.A. (2000) The structural basis of ribosome activity in peptide bond synthesis. *Science*, **289**, 920–930.
7. Khaitovich,P., Mankin,A.S., Green,R., Lancaster,L. and Noller,H.F. (1999) Characterization of functionally active subribosomal particles from *Thermus aquaticus*. *Proc. Natl Acad. Sci. USA*, **96**, 85–90.
8. Weiss,R.L., Kimes,B.W. and Morris,D.R. (1973) Cations and ribosome structure. Effects on the 30S and 50S subunits of replacing bound Mg^{2+} by inorganic cations. *Biochemistry*, **12**, 450–456.
9. Draper,D.E. (1995) Protein–RNA recognition. *Annu. Rev. Biochem.*, **64**, 593–620.
10. Winter,D., Polacek,N., Halama,I., Streicher,B. and Barta,A. (1997) Lead-catalysed specific cleavage of ribosomal RNAs. *Nucleic Acids Res.*, **25**, 1817–1824.
11. Polacek,N. and Barta,A. (1998) Metal ion probing of rRNAs: evidence for evolutionarily conserved divalent cation binding pockets. *RNA*, **4**, 1282–1294.

12. Dorner,S. and Barta,A. (1999) Probing ribosome structure by europium-induced RNA cleavage. *Biol. Chem.*, **380**, 243–251.
13. Conn,G.L., Draper,D.E., Lattman,E.E. and Gittis,A.G. (1999) Crystal structure of a conserved ribosomal protein–RNA complex. *Science*, **284**, 1171–1174.
14. Drygin,D. and Zimmermann,R.A. (2000) Magnesium ions mediate contacts between phosphoryl oxygens at positions 2122 and 2176 of the 23S rRNA and ribosomal protein L1. *RNA*, **6**, 1714–1726.
15. Bayfield,M.A., Dahlberg,A.E., Schulmeister,U., Dorner,S. and Barta,A. (2001) A conformational change in the ribosomal peptidyl transferase center upon active/inactive transition. *Proc. Natl Acad. Sci. USA*, **98**, 10096–10101.
16. Klein,D.J., Moore,P.B. and Steitz,T.A. (2004) The contribution of metal ions to the structural stability of the large ribosomal subunit. *RNA*, **10**, 1366–1379.
17. Stevens,L. and Pascoe,G. (1972) The location of spermine in bacterial ribosomes as indicated by 1,5-difluoro-2,4-dinitrobenzene and by ethidium bromide. *Biochem. J.*, **128**, 279–289.
18. Bernabeu,C., Vazquez,D. and Ballesta,J.P.G. (1978) Proteins associated with rRNA in the *Escherichia coli* ribosome. *Biochim. Biophys. Acta*, **518**, 290–297.
19. Kakegawa,T., Sato,E., Hirose,S. and Igarashi,K. (1986) Polyamine binding sites on *Escherichia coli* ribosomes. *Arch. Biochem. Biophys.*, **251**, 413–420.
20. Amarantos,I., Xaplanteri,M.A., Choli-Papadopoulou,T. and Kalpaxis,D.L. (2001) Effects of two photoreactive spermine analogues on peptide bond formation and their application for labeling proteins in *Escherichia coli* functional ribosomal complexes. *Biochemistry*, **40**, 7641–7650.
21. Xaplanteri,M.A., Andreou,A., Dinos,G.P. and Kalpaxis,D.L. (2003) Effect of polyamines on the inhibition of peptidyltransferase by antibiotics: revisiting the mechanism of chloramphenicol action. *Nucleic Acids Res.*, **31**, 5074–5083.
22. Petropoulos,A.D., Xaplanteri,M.A., Dinos,G.P., Wilson,D.N. and Kalpaxis,D.L. (2004) Polyamines affect diversely the antibiotic potency: insight gained from kinetic studies of the blasticidin S and spiramycin interactions with functional ribosomes. *J. Biol. Chem.*, **279**, 26518–26525.
23. Agrawal,R.K., Penczek,P., Grassucci,R.A., Burkhard,N., Nierhaus,K.H. and Frank,J. (1999) Effect of buffer conditions on the position of tRNA on the 70S ribosome as visualized by cryoelectron microscopy. *J. Biol. Chem.*, **274**, 8723–8729.
24. Jelenc,P.C. and Kurland,C.G. (1979) Nucleoside triphosphate regeneration decreases the frequency of translation errors. *Proc. Natl Acad. Sci. USA*, **76**, 3174–3178.
25. Bartetzko,A. and Nierhaus,K.H. (1988) Mg^{2+}/NH_4^+/polyamine system for polyuridine-dependent polyphenylalanine synthesis with near *in vivo* characteristics. *Methods Enzymol.*, **164**, 650–658.
26. Cohen,S.S. (1998) *A Guide to Polyamines*. Oxford University Press, New York, NY.
27. Fujiwara,K., Bai,G., Kitagawa,T. and Tsuru,D. (1998) Immunoelectron microscopic study for polyamines. *J. Histochem. Cytochem.*, **46**, 1321–1328.
28. Drainas,D. and Kalpaxis,D.L. (1994) Bimodal action of spermine on ribosomal peptidyltransferase at low concentration of magnesium ions. *Biochim. Biophys. Acta*, **1208**, 55–64.
29. Amarantos,I. and Kalpaxis,D.L. (2000) Photoaffinity polyamines: interactions with AcPhe-tRNA free in solution or bound at the P-site of *Escherichia coli* ribosomes. *Nucleic Acids Res.*, **28**, 3733–3742.
30. Kamekura,M., Hamana,K. and Matsuzaki,S. (1987) Polyamine contents and amino acid decarboxylation activities of extremely halophilic archaebacteria and some eubacteria. *FEMS Microbiol. Lett.*, **43**, 301–305.
31. Kakegawa,T., Guo,Y., Chiba,Y., Miyazaki,T., Nakamura,M., Hirose,S., Canellakis,Z.N. and Igarashi,K. (1991) Effect of acetylpolyamines on *in vitro* protein synthesis and on the growth of a polyamine-requiring mutant of *Escherichia coli*. *J. Biochem.*, **109**, 627–631.
32. Tanaka,Y., Kojima,C., Morita,E.H., Kasai,Y., Yamasaki,K., Ono,A., Kainosho,M. and Taira,K. (2002) Identification of the metal ion binding site on an RNA motif from hammerhead ribozymes using (15)N NMR spectroscopy. *J. Am. Chem. Soc.*, **124**, 4595–4601.
33. Batanao,D.R., Altman,R.B. and Klein,T.E. (2003) Microenvironment analysis and identification of magnesium binding sites in RNA. *Nucleic Acids Res.*, **31**, 4450–4460.
34. Amarantos,I., Zarkadis,I.K. and Kalpaxis,D.L. (2002) The identification of spermine binding sites in 16S rRNA allows interpretation of the spermine effect on ribosomal 30S subunit functions. *Nucleic Acids Res.*, **30**, 2832–2843.
35. Clark,E., Swank,R.A., Morgan,J.E., Basu,H. and Matthews,H.R. (1991) Two new photoaffinity polyamines appear to alter the helical twist of DNA in nucleosome core particles. *Biochemistry*, **30**, 4009–4020.
36. Dinos,G., Wilson,D.N., Teraoka,Y., Szaflarski,W., Fucini,P., Kalpaxis,D.L. and Nierhaus,K.H. (2004) Dissecting the ribosomal inhibition mechanisms of edeine and pactamycin: the universally conserved residues G693 and C795 regulate P-site RNA binding. *Mol. Cell*, **13**, 113–124.
37. Nierhaus,K.H. and Dohme,F. (1974) Total reconstitution of functionally active 50S ribosomal subunits from *Escherichia coli*. *Proc. Natl Acad. Sci. USA*, **71**, 4713–4717.
38. Stern,S., Moazed,D. and Noller,H.F. (1988) Structural analysis of RNA using chemical and enzymatic probing monitored by primer extension. *Methods Enzymol.*, **164**, 481–489.
39. Egebjerg,J., Larsen,N. and Garrett,R.A. (1990) Structural map of 23S rRNA. In Hill,W.E., Dahlberg,A., Garrett,R.A., Moore,P.B., Schlessinger,D. and Warner,J.R. (eds), *The Ribosome: Structure, Function, and Evolution*. American Society for Microbiology, Washington, pp. 168–178.
40. Agrawal,R.K. and Burma,D.P. (1996) Sites of ribosomal RNAs involved in the subunit association of tight and loose couple ribosomes. *J. Biol. Chem.*, **271**, 21285–21291.
41. Merryman,C., Moazed,D., Daubresse,G. and Noller,H.F. (1999) Nucleotides in 23S rRNA protected by the association of 30S and 50S ribosomal subunits. *J. Mol. Biol.*, **285**, 107–113.
42. Kutay,U.R., Spahn,C.M.T. and Nierhaus,K.H. (1990) Similarities and differences in the inhibition patterns of thiostrepton and viomycin: evidence for two functionally different populations of P sites when occupied with AcPhe-tRNA. *Biochem. Biophys. Acta*, **1050**, 193–196.
43. Brandi,L., Marzi,S., Fabbretti,A., Fleischer,C., Hill,W.F., Gualerzi,C.O. and Lodmell,J.S. (2004) The translation initiation functions of IF2: targets for thiostrepton inhibition. *J. Mol. Biol.*, **335**, 881–894.
44. Igarashi,K. and Kashiwagi,K. (2000) Polyamines: mysterious modulators of cellular functions. *Biochem. Biophys. Res. Commun.*, **271**, 559–564.
45. Koculi,E., Lee,N.-K., Thirumalai,D. and Woodson,S.A. (2004) Folding of the Tetrahymena ribozyme by polyamines: importance of counterion valence and size. *J. Mol. Biol.*, **341**, 27–36.
46. Gautheret,D., Konings,D. and Gutell,R.R. (1995) G.U base pairing motifs in ribosomal RNA. *RNA*, **1**, 807–814.
47. Bibillo,A., Figlerowicz,M. and Kierzek,R. (1999) The non-enzymatic hydrolysis of oligoribonucleotides VI. The role of biogenic polyamines. *Nucleic Acids Res.*, **27**, 3931–3937.
48. Harms,J., Schluenzen,F., Zarivach,R., Bashan,A., Gat,S., Agmon,I., Bartels,H., Franceschi,F. and Yonath,A. (2001) High resolution structure of the large ribosomal subunit from a mesophilic eubacterium. *Cell*, **107**, 679–688.
49. Aagaard,C. and Douthwaite,S. (1994) Requirement for a conserved, tertiary interaction in the core of 23S ribosomal RNA. *Proc. Natl Acad. Sci. USA*, **91**, 2989–2993.
50. Stelzl,U. and Nierhaus,K.H. (2001) A short fragment of 23S rRNA containing the binding sites for two ribosomal proteins, L24 and L4, is a key element for rRNA folding during early assembly. *RNA*, **7**, 598–609.
51. Wilson,D.N., Blaha,G., Connell,S.R., Ivanov,P.V., Jenke,H., Stelzl,U., Teraoka,Y. and Nierhaus,K.H. (2002) Protein synthesis at atomic resolution: mechanistics of translation in the light of highly resolved structures for the ribosome. *Curr. Protein Pept. Sci.*, **3**, 1–53.
52. Wilson,K.S. and Nechifor,R. (2004) Interactions of translational factor EF-G with the bacterial ribosome before and after mRNA translocation. *J. Mol. Biol.*, **337**, 15–30.
53. Agmon,I., Amit,M., Auerbach,T., Bashan,A., Baram,D., Bartels,H., Berisio,R., Greenberg,I., Harms,J., Hansen,H.A.S. *et al.* (2004) Ribosomal crystallography: a flexible nucleotide anchoring tRNA translocation, facilitates peptide-bond formation, chirality discrimination and antibiotics synergism. *FEBS Lett.*, **567**, 20–26.
54. Rawat,U.B.S., Zavialov,A.V., Sengupta,J., Valle,M., Grassucci,R.A., Linde,J., Vestergaard,B., Ehrenberg,M. and Frank,J. (2003) A cryo-electron microscopic study of ribosome-bound termination factor RF2. *Nature*, **421**, 87–90.

55. Mueller,F., Sommer,I., Baranov,P., Matadeen,R., Stoldt,M., Wöhnert,J., Görlach,M., van Heel,M. and Brimacombe,R. (2000) The 3D arrangement of the 23S and 5S rRNA in the *Escherichia coli* 50S ribosomal subunit based on a cryo-electron microscopic reconstruction at 7.5 A resolution. *J. Mol. Biol.*, **298**, 35–59.
56. Bullard,J.M., van Waes,M.A., Bucklin,D.J. and Hill,W.E. (1995) Regions of 23S ribosomal RNA proximal to transfer RNA bound at the P and E sites. *J. Mol. Biol.*, **252**, 572–582.
57. Polacek,N., Gomez,M.J., Ito,K., Xiong,L., Nakamura,Y. and Mankin,A. (2003) The critical role of the universally conserved A2602 of 23S ribosomal RNA in the release of the nascent peptide during translation termination. *Mol. Cell*, **11**, 103–112.
58. Sievers,A., Beringer,M., Rodnina,M.V. and Wolfender,R. (2004) The ribosome as an entropy trap. *Proc. Natl Acad. Sci. USA*, **101**, 7897–7901.
59. Rodriguez-Fonseca,C., Amils,R. and Garrett,R.A. (1995) Fine structure of the peptidyl transferase centre on 23S-like rRNAs deduced from chemical probing of antibiotic-ribosome complexes. *J. Mol. Biol.*, **247**, 224–235.
60. Lancaster,L., Kiel,M.C., Kaji,A. and Noller,H.F. (2002) Orientation of ribosome recycling factor in the ribosome from directed hydroxyl radical probing. *Cell*, **111**, 129–140.
61. Scarlett,D.-J.G., McCaughan,K.K., Wilson,D.N. and Tate,W.P. (2003) Mapping functionally important motifs SPF and GGQ of the decoding release factor RF2 to the *Escherichia coli* ribosome by hydroxyl radical footprinting. Implications for macromolecular mimicry and structural changes in RF2. *J. Biol. Chem.*, **278**, 15095–15104.
62. Klaholz,B.P., Myasnikov,A.G. and van Heel,M. (2004) Visualization of release factor 3 on the ribosome during termination of protein synthesis. *Nature*, **427**, 862–865.
63. Schlünzen,F., Harms,J.M., Franceschi,F., Hansen,H.A., Bartels,H., Zarivach,R. and Yonath,A. (2003) Structural basis for the antibiotic activity of ketolides and azalides. *Structure*, **11**, 329–338.